Biological and biogeochemical methods for estimating bio-irrigation: a case study in the Oosterschelde estuary.

Emil De Borger[1,2], Justin Tiano[2,1], Ulrike Braeckman[1], Tom Ysebaert[2,3], Karline Soetaert[2,1].

[1]Ghent University, Department of Biology, Marine Biology Research Group, Krijgslaan 281/S8, 9000 Ghent, Belgium
[2]Royal Netherlands Institute of Sea Research (NIOZ), Department of Estuarine and Delta Systems, and Utrecht University, Korringaweg 7, P.O. Box 140, 4401 NT Yerseke, The Netherlands
[3]Wageningen Marine Research, Wageningen University & Research, Wageningen, Netherlands

Correspondence to : Emil De Borger (emil.de.borger@nioz.nl)

Abstract

Bio-irrigation, the exchange of solutes between overlying water and sediment by benthic organisms, plays an important role in sediment biogeochemistry. Bio-irrigation is either quantified based on tracer data or, a community (bio-) irrigation potential (IPc) can be derived based on biological traits. Both these techniques were applied in a seasonal study of bio-irrigation in subtidal and intertidal habitats in a temperate estuary. The combination of a tracer time series with high temporal resolution and a mechanistic model allowed to simultaneously estimate the pumping rate, and the sediment attenuation, a parameter that determines irrigation depth. We show that although the total pumping rate is similar in both intertidal and subtidal areas, there is deeper bio-irrigation in intertidal areas. This is explained by higher densities of bio-irrigators such as *Corophium sp.*, *Heteromastus filiformis* and *Arenicola marina* in the intertidal, as opposed to the subtidal. The IPc correlated more strongly with the attenuation coefficient than the pumping rate, which highlights that the IPc index reflects more the bio-irrigation depth rather than the rate.

1 Introduction

Bio-irrigation is the process in which benthic organisms actively or passively exchange sediment porewater solutes with the overlying water column as a result of burrowing, pumping (ventilation) and feeding activities (Kristensen et al., 2012). This exchange plays an important role in marine and lacustrine sediment biogeochemistry, as oxygen rich water is brought into an otherwise sub- or anoxic sediment matrix. This allows for aerobic degradation processes to take place, as well as the reoxidation of reduced substances (Aller and Aller, 1998; Kristensen, 2001), and enables sediment dwelling organisms to forage and live in the otherwise anoxic deeper sediment layers (Olaffson, 2003; Braeckman et al., 2011). By extending the sediment- water interface in the vertical dimension, burrowing organisms increase the exchange surface, especially when burrow water is refreshed by ventilation activities. This enhances nutrient exchange (Quintana et al., 2007), and increases degradation rates (Na et al., 2008). Sedimentary bio-irrigation is the result of the combined actions of a multitude of organisms sharing the same

habitat. Some organisms such as the smaller meiofauna, located close to the sediment water interface, exchange only small amounts of solutes, but due to their high densities their activities affect the sediment porosity and as such exert a significant effect on sediment-water exchanges in the top layers of the sediment (Aller and Aller, 1992; Rysgaard et al., 2000). On the opposite end of the spectrum are larger infaunal species such as the burrowing shrimp *Upogebia pugettensis* (Dana, 1852) which constructs burrows that extend up to 1 m into the sediment and that actively ventilates these burrows using its pleiopods (D'Andrea and DeWitt, 2009). These deep burrows substantially extend the oxic sediment-water interface into the sediment, influencing the associated microbial respiration through various pathways (Nielsen et al., 2004). The effect of bio-irrigation also depends on the sediment matrix. In muddy sediments, where permeability is low, bio-irrigation impacts are localized close to the burrow wall, as the transport of solutes radiating from the burrows is governed by diffusion (Aller, 1980). In sandy, more permeable sediments the pressure gradients caused by ventilation activities induce water flows through the surrounding sediments, thus affecting the sediment matrix further away from the burrow walls (Meysman et al., 2005; Timmermann et al., 2007). Therefore, the effects of bio-irrigation depend on a combination of the species community, species' individual behavior including ventilation activity, the depths at which they occur, and the sediment matrix they inhabit.

Bio-irrigation can be quantified with biogeochemical methods, or a qualitative estimate can be calculated by an index of bio-irrigation based on biological information. The biogeochemical methods estimate the exchange rates of a tracer substance (usually inert) between the overlying water and the sediment, by fitting a linear model (De Smet et al., 2016; Mestdagh et al., 2018; Wrede et al., 2018), or a quasi-mechanistic model (Berelson et al., 1998; Andersson et al., 2006) through measured concentration time series. A linear decrease returns the rate of disappearance of the tracer from the water column over a given time period, but it gives little information on the bio-irrigation process itself, e.g. what is the actual pumping rate, and where in the sediment are solutes exchanged. While sometimes the depth distribution of the tracer in the sediment is characterized post-experiment to obtain this information (Martin and Banta, 1992; Berg et al., 2001; Hedman et al., 2011), this step is often overlooked. By increasing the temporal resolution of the tracer concentration measurements, an exponential decrease can be fitted through the data, from which a bio-irrigation rate can be derived which is independent of the length of the experiment (Meysman et al., 2006; Na et al., 2008). For these applications fluorescent tracers are used, as they can be monitored *in-situ*, and the measurement is instantaneous. So far, this method has been applied in controlled settings, but not yet in field applications.

The index approach starts with the quantification of the abundance and biomass of organisms inhabiting the sediment, and an assessment of how these organisms bio-irrigate. The latter is done based on a set of life history traits which are assumed to contribute to bio-irrigation: the type of burrow they inhabit, their feeding type and their burrowing depth. Species are assigned one trait score for each trait, independent of the biological context in which they occur (but see Renz et al. (2018)). The species biomass and abundance, combined with their trait scores are then used to derive an index that represents the community (bio-) irrigation potential (BIPc and IPc in Renz et al., 2018 and Wrede et al., 2018 respectively), a similar practice to what is done for bioturbation with the community bioturbation potential (BPc; Queirós et al., 2013). The inherent assumptions of this approach are that bio-irrigation activity increases linearly with the number of organisms, and scales with their mean weight

through a metabolic scaling factor. The advantage of biologically-based indices is that large datasets of benthic communities are currently available (e.g. Craeymeersch et al., 1986; Degraer et al., 2006; Northeast Fisheries Science Center, 2018), so that these data have great potential to derive information on the temporal and spatial variability of bio-irrigation. However, in contrast to the related bioturbation potential (Solan et al., 2004), the classification of sediments according to their bio-irrigation potential is a very recent endeavor, and the underlying mechanistic basis of these indices, i.e. what they actually describe, should be explored further. As a first step in this direction, the IPc index of Wrede et al. (2018) has been calibrated against bromide uptake rates for selected individual species and communities in the German Bight of the North Sea.

The aim of the current study was to compare bio-irrigation rate measurements with an index of bio-irrigation in natural sediments of a temperate estuarine system, the Oosterschelde. Samples were collected across different seasons in three subtidal and three intertidal sites with different benthic communities, and sediments varying from muddy to sandy. Bio-irrigation rates were derived by fitting a novel mechanistic model through a quasi-continuous time series of a fluorescent tracer, while biological information was used to calculate the IPc index.

2 Materials and methods

2.1 Sampling

Field samples were collected in the Oosterschelde (SW Netherlands) from August 2016 to December 2017 (Fig. 1). Six sites (3 subtidal, 3 intertidal) were selected based on results from previous sampling efforts, to reflect the variability in inundation time and sediment composition present in this area (Table 1). The intertidal sites Zandkreek (N 51.55354°, E 3.87278°), Dortsman (N 51.56804°, E 4.01425°) and Olzendenpolder (N 51.46694°, E 4.072694°) were sampled by pressing two cylindrical PVC cores (14.5 cm Ø, 30 cm height) in the sediment at low tide up to a depth of 20 cm at most, and extracting them from the sediment. The subtidal sites Hammen (N 51.65607°, E 3.858717°), Viane (N 51.60675°, E 3.98501°), and Lodijksegat (N 51.48463°, E 4.166001°) were sampled in the same way, but sediment was retrieved from duplicate deployments of a NIOZ box-corer aboard the Research Vessel Delta. In total 70 individual cores in the intertidal, and 47 in the subtidal were retrieved. Sediment permeability has a strong influence on bio-irrigation rates (Aller, 1983; Meysman et al., 2006). Sediment permeability was not directly measured, but additional samples for sediment characteristics relating to this property (grain size distribution and porosity) were taken from the top 2 cm of sediment at each site, using a cut-off syringe. From the same samples a subsample was collected for determining the chlorophyll *a* content, and C/N ratios in the sediment, as measures of food availability and quality respectively.

After transportation to the laboratory, the cores were placed into seawater tanks in a climate room set to the average water temperature of the month in which the samples were taken (Table 1: seasonal averages). By adding 0.45 µm filtered Oosterschelde water, the overlying water height was brought to at least 10 cm, and air stones and a stirring lid (central Teflon coated magnet stirrer) with sampling ports were used to keep the water oxygenated. The sediment cores were left to acclimatize for 24 to 48 hours before starting the irrigation experiment. For the irrigation measurements, a stock solution of 1 mg L^{-1}

uranine (sodium fluoresceine - $C_{20}H_{10}NaO_5^-$) was prepared by dissolving 1 mg of uranine salts into 1 L of 0.45 µm filtered Oosterschelde water. Short experiments were performed to assess possible interactions between the tracer, and the incubation cores and stirring devices (Supplement). To start the experiment 30 to 40 mL of the stock solution was added to the overlying water to achieve a starting concentration of uranine of about 10 µg L^{-1}. The concentration of the fluorescent tracer was subsequently measured every 30 seconds for a period of at least 12 hours with a fluorometer (Turner designs cyclops 6) placed in the water column through a sampling port in the stirring lid of the core, ± 6 cm below the water surface. After the measurement, the sediment was sieved over a 1 mm sieve and the macrofauna was collected and stored in 4% buffered formalin for species identification and abundance and biomass determination.

Sediment grain size was determined by laser diffraction on freeze dried and sieved (< 1 mm) sediment samples in a Malvern Mastersizer 2000 (McCave et al., 1986). Water content was determined as the volume of water removed by freeze drying wet sediment samples. Sediment porosity was determined from water content and solid phase density measurements, accounting for the salt content of the pore water. Chl *a* was extracted from the freeze dried sediment sample using acetone, and quantified through UV spectrophotometry (Ritchie, 2006). The C/N ratio was calculated from total C and N concentrations, determined using an Interscience Flash 2000 organic element analyser.

2.2 Model

The exchange of a tracer (*T*) between the sediment and the overlying water is described in a (vertical) one-dimensional mechanistic model, that includes molecular diffusion, adsorption to sediment particles, and bio-irrigation. The bio-irrigation is implemented as a non-local exchange in which a pumping rate (*r)* exponentially decays with distance from the sediment surface (z). This exponential decay mimics the depth dependent distribution of faunal biomass often found in sediments (Morys et al., 2017) and the associated decreasing amount of burrow cross-sections with depth (Martin and Banta, 1992; Furukawa et al., 2001).

The mass balance for a dissolved tracer (*T*, Eq. 1) and the adsorbed tracer (*A*, Eq. 2) in an incubated sediment with height h_s, at a given depth (*z*, cm) and time (*t*, hours) in the sediment is:

$$\frac{\partial T_z}{\partial t} = \frac{1}{\varphi_z} \cdot \frac{\partial}{\partial z}\left[D_s \varphi_z \frac{\partial T_z}{\partial z}\right] + r \frac{e^{-az}}{\int_0^{h_S} e^{-az}\, dz} \cdot (T_{OW} - T_z) - k \cdot (Eq_A \cdot T_z - A_z) \cdot \rho \cdot \frac{(1-\varphi_z)}{\varphi_z} \quad (1)$$

$$\frac{\partial A_z}{\partial t} = k \cdot (Eq_A \cdot T_z - A_z) \quad (2)$$

In this equation φ_z is sediment porosity (-), and ρ is sediment density (g cm^{-3}).

In the equation for *T* (Eq. 1), the first term represents transport due to molecular diffusion, where D_s is the sediment diffusion coefficient (cm^2 h^{-1}). The second term represents the exchange of tracer between the water column (T_{OW}) and any sediment depth *z* due to irrigation, where the exchange rate decreases exponentially as modulated by the attenuation coefficient *a* (cm^{-1}). The exponential term is scaled with the integrated value, so that the exchange rate *r* reflects the total rate of bio-irrigation, expressed in (cm h^{-1}).

The loss term for the tracer by adsorption (third term) depends on the deviation from the local equilibrium of the tracer with the actual adsorbed fraction on the sediment and with parameters k (h^{-1}), the rate of adsorption, and Eq_A, the adsorption equilibrium (ml g^{-1}).

The dissolved tracer concentration in the water column (T_{OW}) (Eq. 3) decreases by the diffusive flux into the sediment and the integrated irrigation flux, corrected for the thickness of the overlying water (h_{OW}, cm):

$$\frac{\partial T_{OW}}{\partial t} = \frac{1}{h_{OW}}\left(-D_s\varphi_0 \frac{\partial T_z}{\partial z}\Big|_{z=0} - \int_0^{h_S} r.\frac{e^{-az}}{\int_0^{h_S} e^{-az}\,dz}(T_{OW} - T_z)dz\right) \quad (3)$$

The concentration of A in the overlaying water equals 0.

The model was implemented in FORTRAN and integrated using the ode.1D solver from the R package deSolve (Soetaert et al., 2010; R Core Team, 2013). The sediment was subdivided into 50 layers; thickness of the first layer set equal to 0.5 mm and then exponentially increasing until the total sediment modelled was equal to the sediment height in each laboratory experiment.

2.3 Model fitting

Most of the input parameters of the model were constrained by physical measurements. Sediment porosity ϕ and specific density ρ (g cm^{-3}) were derived from sediment samples taken alongside the cores in the field. The adsorption equilibrium Eq_A (in ml g^{-1}) was determined from batch adsorption experiments (See supplementary data). The modelled sediment height (h_S) and water column height (h_{OW}) were set equal to the experimental conditions. This left two parameters governing the bio-irrigation rate to be estimated by model fitting: r, the integrated pumping rate and a, the attenuation coefficient. Fitting of the model to the experimental data was done with the R package FME (Soetaert and Petzoldt, 2010). First an identifiability analysis was performed to investigate the certainty with which these parameters could be derived from model fitting given the experimental data. This entails a local sensitivity analysis to quantify the relative effects of said parameters on model output, and a collinearity analysis to test whether parameters were critically correlated, and thus not separately identifiable, or the opposite. Then both parameters were estimated by fitting the model to each individual tracer time series through minimization of the model cost (the weighted sum of squares) using the pseudo-random search algorithm (Price, 1977) followed by the Levenberg-Marquardt algorithm. Lastly, a sensitivity analysis was performed to calculate confidence bands around the model output, based on the parameter covariance matrix derived from the fitting procedure (Soetaert and Petzoldt, 2010).

2.4 Calculation of IP_c and BP_c

The retrieved benthic macrofauna were identified down to lowest possible taxonomic level, counted and their ash-free dry weight (gAFDW m^{-2}) was converted from blotted wet weight according to Sistermans et al. (2006). Based on the species abundance and biomass, the irrigation potential of the benthic community in a sediment core (IPc, Eq. 4) was calculated as described in Wrede et al. (2018):

$$IP_c = \sum_{i=1}^{n} \left(\frac{B_i}{A_i}\right)^{0.75} \cdot A_i \cdot BT_i \cdot FT_i \cdot ID_i \quad (4)$$

in which B_i represents the biomass (gAFDW m^{-2}), A_i the abundance (ind. m^{-2}) of species *i* in the core, and BT_i, FT_i and ID_i are descriptive numerical scores for the species burrowing type, feeding type and injection pocket depth respectively. The values for FT_i, BT_i and ID_i were the same as applied by Wrede et al. (2018). If not available, values were assigned based on the closest taxonomic relative, with possible adjustments to correct for size differences and feeding type as taxonomic relation is not always a measure for similarity in traits.

The community bioturbation potential (BP_c, Eq. 5) was calculated as described in Solan et al. (2004):

$$BP_c = \sum_{i=1}^{n} \left(\frac{B_i}{A_i}\right)^{0.5} \cdot A_i \cdot M_i \cdot R_i \quad (5)$$

with M_i the mobility score and R_i the reworking score for species *i* from Queirós et al. (2013). Note that the biomass *B* in this case is the blotted wet weight of the organisms.

2.5 Data analysis

Differences in model derived pumping rates *r* and attenuation coefficient *a* between subtidal and intertidal were tested using a two-sided T-test (using a significance level of 0.05). For further multivariate analysis, species densities, biomass, and estimated irrigation parameters were averaged per station, and per season (Fig. 2) since not all six stations were sampled on the same date. The patterns in abiotic conditions, species composition and bio-irrigation rates were analysed using ordination techniques for multivariate datasets as described in Thioulouse et al.(2018), and implemented in the ade4 R package (Dray and Dufour, 2015). In this procedure, a coinertia analysis and permutation first tests the null hypothesis that there is no significant relationship between environmental variables and species densities, and then the correlation of the bio-irrigation rates to the environment-species data is assessed. In a first step, the species data matrix was processed by centered Principle Component Analysis (PCA). For this the species relative densities were used to emphasize the specific functional role of some species within the communities (Beauchard et al., 2017) and to reduce the effects of heavy outliers. Secondly the environmental variable matrix was processed by Multiple Correspondence Analysis (MCA; Tenenhaus and Young (1985). This technique can account for non-linear relationships between variables, but requires all variables to be categorical. Sediments were categorized based on grain size into the Udden-Wentworth scale (Wentworth, 1922) of silt (< 63 µm), very fine sand (> 63 µm, < 125 µm) and fine sand (> 125 µm, < 250 µm); the Chl a content was categorized to distinguish sites with low (< 8 µg g^{-1}), intermediate (8-16 µg g^{-1}) and high (> 16 µg g^{-1}) chlorophyll content. Two abiotic variables were already categorical: habitat type (intertidal versus subtidal) and season. Sediment porosity and C/N ratio were not used in the analysis given the small range within these data (Table 2). In a third step, the two ordinations were combined in a Co-Inertia Analysis (CoIA; Dray et al. (2003)), to explore the co-structure between the species and the environmental variables. The significance of the overall relationship (the co-structure of species and environment) between the two matrices was tested by a Monte-Carlo procedure based on 999 random permutations of the row matrices (Heo and Gabriel, 1998). Finally, the correlations between the response variables relating to irrigation (estimated irrigation parameters, calculated IPc, BPc) and the two axes of the co-

inertia analysis were assessed using the Pearson correlation coefficient assuming a significance level of 0.05. Results are expressed as mean ± sd.

3 Results

3.1 Environmental variables

Sediment descriptors are summarized in Table 2. Chlorophyll a concentrations in the upper 2 cm of the sediment varied from 3.76 ± 2.43 µg g^{-1} in Hammen to 20.60 ± 4.19 µg g^{-1} in Zandkreek and were higher in the intertidal (13.34 ± 6.53 µg g^{-1}) than in the subtidal (5.88 ± 4.20 µg g^{-1}). In the intertidal, the median grain size (d50) and silt content ranged from 59 µm with 52% silt to 140 µm with 0% silt. In the subtidal the range in grain size was broader, from 53 µm with 63% silt to 201 µm with 24% silt. The C/N ratio (mol mol^{-1}) was similar for all sites (9.3 ± 1.0 – 12.3 ± 1.4) with the exception of Dortsman, where values were lower (6.5 ± 1.2). Dortsman was also the site where the organic carbon content was lowest (0.07 ± 0.02 %). The organic carbon content increased with silt content, to highest values in the most silty station Viane (1.16 ± 0.36 %).

3.2 Macrofauna

In total, 60 species were identified in the 6 different stations (Table 3). Species abundances in the intertidal were generally one, sometimes two orders of magnitude higher than in the subtidal (see Fig. 2: a, b for seasonal species density and biomass data). In the intertidal, maximum abundances were observed in Dortsman in autumn and spring, with peak values of 15202 ± 4863 and 16054 ± 13939 ind. m^{-2} respectively, mainly due to high abundances of the amphipods *Corophium sp.* and *Bathyporeia* sp. (respective peak values of 9957 ± 4465 and 3934 ± 3087 ind. m^{-2}). Subtidal densities varied less and were highest in Lodijksegat in autumn and summer (peak values of 661 ± 502 and 790 ± 678 ind. m^{-2} respectively). Faunal biomass was larger in the subtidal (22.31 ± 26.42 gAFDW m^{-2}) as opposed to the intertidal (10.51 ± 8.59 gAFDW m^{-2}), with peak summer values at the subtidal Lodijksegat station (39.90 ± 34.87 gAFDW m^{-2}) coinciding with high abundances (972 ± 172 ind. m^{-2}) of the common slipper limpet *Crepidula fornicata* (Linnaeus, 1758).

3.3 Bio-irrigation rates

A typical time series of uranine concentrations shows the tracer to exponentially decrease towards a steady value (Fig. 3a). The pumping rate and irrigation attenuation (parameters *r* and *a*) have an opposite effect on tracer concentrations in the overlying water, but a collinearity analysis (Soetaert and Petzoldt, 2010) showed that these two parameters could be fitted simultaneously. The attenuation coefficient *a* affects the depth of the sediment which is irrigated, with larger values of *a* resulting in more shallow bio-irrigation. Higher pumping rates, *r*, entail a faster removal of the tracer from the water. Compared to the parameters *r* and *a*, the rate of adsorption, *k* had a 1000-fold weaker effect on the outcome. Its value was set to 1 (h^{-1}) implying that it takes about 1 hour for the sediment adsorbed tracer fraction to be in equilibrium with the porewater tracer fraction.

In 11 out of 117 cases the fitting procedure yielded fits for which both the attenuation coefficient *a* and the pumping rate *r* were not significantly different from 0 and for which bio-irrigation was thus assumed to be absent. These were predominantly observed in November and December (7 out of 11 non-significant fits) and in these cases the tracer concentration did not notably change but rather fluctuated around a constant value.

The fitted irrigation rates and attenuation coefficients did not show clear seasonal trends in the intertidal stations (Fig. 2). In the subtidal stations, irrigation rates were lowest in autumn, and highest in winter (Fig. 2c). There was no significant difference in irrigation rates between the subtidal (0.547 ± 1.002 mL cm^{-2} h^{-1}) and intertidal (0.850 ± 1.157 mL cm^{-2} h^{-1}) (Welch two-sample T-test: $p = 0.708$). Seasonally averaged irrigation rates were highest at Lodijksegat in winter (1.693 ± 1.375 mL cm^{-2} h^{-1}), whereas in autumn at that same station they were lowest (0.091 ± 0.078 mL cm^{-2} h^{-1}). The model derived attenuation coefficients were significantly higher in the subtidal (2.387 ± 3.552 cm^{-1}) than in the intertidal (0.929 ± 1.793 cm^{-1}) (Welch two-sample T-test: $p = 0.041$).

3.4 Co-inertia analysis

The first and second axes of the co-inertia analysis (CoiA) explained 57% and 19% of the variance in the dataset respectively (histogram inset Fig. 4a). The Monte-Carlo permutation test resulted in a significant RV coefficient (the multivariate generalization of the squared Pearson correlation coefficient) of 0.62 ($p < 0.001$), showing that the species data and the environmental data are significantly correlated. Both the first and second axes of the MCA performed on the environmental parameters and of the PCA performed on the species community were correlated, indicated by high Pearson correlation coefficients (Figure 4: Summary of the coinertia analysis (CoIA). (a) Co-structure between abiotic samples (circles) and species samples (arrow tips); grey circles “D”, “O”,“Z” for intertidal sites Dortsman, Olzendenpolder and Zandkreek respectively; white circles “H”, “L”, “V” for subtidal sites Hammen, Lodijksegat and Viane respectively. Arrow length corresponds to the dissimilarity between the abiotic data and the species data (the larger the arrow, the larger the dissimilarity). Pearson’s correlation between the circle and arrow tip coordinates on the first axis: r = 0.95, p < 0.001; on the second axis, r = 0.92, p < 0.001. Sites are more similar in terms of environmental conditions (circles), or species (arrow tips), when they group closer together. Inset: eigenvalue diagram of the co-structure; first axis explains 57%, second axis explains 19% of the variation in the dataset. (b) MBA based on environmental variables. (c) Species projections (dark arrows) and projected response variables (bio-irrigation parameters and bioturbation and bio-irrigation index) onto the co-inertia axes (grey arrows). The directions of arrows in figures b and c corresponds to the directions in which stations are grouped in terms of abiotic data (circles) and species composition (arrow tips) in figure a.

4a; for the first axis: $r = 0.95$, $p < 0.001$; for the second axis: $r = 0.92$, $p < 0.001$). In the MCA of the environmental variables, the first axis reflected mainly a grain size gradient from very fine sandy to silty (Fig. 4b), with subtidal sites Lodijksegat (L) and Hammen (H) on the very fine sandy end, and the intertidal site Zandkreek (Z) in the high silt end (Fig. 4a). The Chl *a* content and the immersion type (intertidal *vs* subtidal) were the main factors associated with axis 2. This axis separated the subtidal station Viane (V) from the intertidal stations Dortsman (D) and Olzendenpolder (O) (Fig. 4a). Of the different seasons,

only summer correlated to the second axis. The PCA of the relative species abundances showed that in more fine sandy subtidal stations species such as the reef forming *Mytilus edulis* (Linnaeus, 1758), and *Lanice conchilega* (Pallas 1766) were found (Fig. 4c). The species *Corophium sp*. and *Peringia ulvae* (Pennant, 1777) dominated in the intertidal, while *Ophiura ophiura* (Linnaeus, 1758) and *Nephtys hombergii* (Lamarck, 1818) were mainly found in the subtidal.

The correlation tests resulted in significant correlations between the first and the second axes of the co-inertia analysis (CoiA) with the BPc (axis 1: $r = 0.54$, $p = 0.008$; axis 2: $r = 0.65$, $p = < 0.001$), and between the first CoiA axis and the IPc (axis 1: $r = 0.78$, $p = < 0.001$; Fig. 4c; see Table 4 for full correlation statistics). Values for these indices are highest in the intertidal samples (Dortsman) and lowest in the subtidal, high Chl *a* samples (Viane), where also respectively the highest and lowest species densities were recorded. The attenuation coefficient *a*, was significantly and negatively correlated with the second axis ($r = -0.57$, $p = 0.005$). The attenuation coefficient increased in the opposite direction of the BPc and IPc indices (Fig. 4c). No significant correlations were found for the model derived pumping rate *r* (axis 1: $r = -0.35$, $p = 0.107$; axis 2: $r = 0.263$, $p = < 0.226$). The pumping rate increased towards the intermediate – low Chl *a* samples, almost perpendicular to both the IPc/BPc arrows and the attenuation coefficient (Fig. 4c).

4 Discussion

4.1 Advantages of mechanistic modelling

Bio-irrigation is a complex process with profound effects on sediment biogeochemistry (Aller and Aller, 1998; Kristensen, 2001). For a better understanding of how bio-irrigation affects the sediment matrix, and to construct indices of irrigation based on species composition and life history traits, it is crucial to understand the mechanistic bases of the process. This is the first study in which continuous measurements of a tracer substance, and a mechanistic model have been combined to study the bio-irrigation behaviour of species assemblages across a range of estuarine habitats. In bio-irrigation experiments, the tracer concentration in the overlying water decreases as it is diluted through mixing with porewater from the sediment. Initially, the sediment porewater is devoid of tracer, so that the dilution of the overlying water concentration is maximal. As the sediment itself becomes charged with tracer, the effect of sediment-water exchange on the bottom water concentration will decrease until the tracer concentration in the bio-irrigated part of the sediment and bottom water concentration are equal, and a quasi-steady state is achieved in which only molecular diffusion further slowly redistributes the tracer in the sediment. This verbal description of a bio-irrigation experiment shows that there are two important aspects to the data: the rate of bio-irrigation determines the initial decrease of tracer and how quickly the steady state will be reached, while the sediment volume over which bio-irrigation occurs determines the difference between initial and ultimate water column tracer concentrations at steady state.

The 1-D mechanistic model applied to our data comprises both these aspects, which are encompassed in two parameters: the integrated rate of bio-irrigation (*r*), and the attenuation coefficient (*a*) that determines the irrigation depth. In model simulations, the differences between fast and slow pumping rates mainly manifest themselves in the first part of the time series,

while differences in irrigation depths are mainly discernable after several hours (Fig. 3b). This adds nuance to the interpretation of bio-irrigation rates, as similar irrigation rates may have divergent effects on sediment biogeochemistry when the depth over which solutes are exchanged differs. We have shown here that this nuance is at play in the Oosterschelde, where model derived pumping rates are very similar in subtidal and intertidal sediments, but the attenuation coefficient was higher for subtidal sites than for intertidal sites, implying a more shallow bio-irrigation pattern in the former. It should be noted that, as the incubation chambers contained at most 20 cm of sediment, the effects of individuals living deeper (e.g. larger *A. marina*, or *N. latericeus*) were not included in the incubations, and thus these were not accounted for in our estimates of bio-irrigation. This means that the bio-irrigation patterns described are only applicable to the upper 20 cm of the sediment.

Our tracer time series were measured at sufficiently high resolution (0.033 Hz), and for a sufficiently long time so that both the initial decrease, and the concentration to which the tracer converges were recorded. Indeed, identifiability analysis, a procedure to discover which model parameters can be estimated from data (Soetaert and Petzoldt, 2010) showed that the information in our data was sufficient to estimate these two parameters (r and a) with high confidence. This represents a significant improvement over discrete tracer measurements, from which deriving information of the depth distribution of irrigation is problematic (Andersson et al., 2006). Other data and/or models may not be able to derive these two quantities. Often bio-irrigation is estimated from linear fits through scarce (≤ 5 measurements) tracer concentration measurements (De Smet et al., 2016; Mestdagh et al., 2018; Wrede et al., 2018). This procedure is mainly applied when bromide is used as a tracer, as concentrations of this substance need to be measured in an elemental analyser, a procedure which, for practical reasons, does not allow quasi-continuous measurements from the same sample. This has a major drawback, as the linearization of the exponential decrease will clearly underestimate the pumping rates, and it will be influenced by the (unknown) tracer depth (Fig. 3). Indeed, these linear fit methods are sensitive to the chosen duration of the experiment, and results based on a time series of 6 hours will not give the same results as those based on a 12 hour measurement.

4.2 Spatio-temporal variability in bio-irrigation

Our data show that although total pumping rates are similar in the subtidal and intertidal sediments of the Oosterschelde, irrigation is shallower in the subtidal, as indicated by the higher attenuation coefficient (Fig. 2c, d). The species community in the subtidal that is responsible for pumping is less dense, but (on average) the biomass is higher than in the intertidal (Table 4). In Viane, the site where bio-irrigation is lowest, only two species occur, *Ophiura ophiura* (Linneaus 1758), and *Nephtys hombergii*, and neither are typically associated with bio-irrigation, although *O. ophiura* can significantly disturb the sediment surface, inducing shallow irrigation (Fig. 4c). The other two subtidal stations harbor two polychaete species that have been found to be prominent bio-irrigators: *Lanice conchilega* (Lodijksegat) and *Notomastus latericeus* (Sars 1851) (both Lodijksegat and Hammen). The sand mason worm *L. conchilega* lives in tubes constructed from shell fragments and sand particles which extend down to 10-15 cm (in the study area) and significantly affects the surrounding biogeochemistry (Forster and Graf, 1995; Braeckman et al., 2010). Highest densities of this species were observed in autumn at Lodijksegat, but interestingly this coincided with lowest bio-irrigation values for this station (Table 2: densities = 375 ± 22 ind m^{-2}; Fig. 2c: bio-irrigation = 0.091

± 0.176 mL cm^{-2} h^{-1}). High densities of *C. fornicata*, an epibenthic gastropod, in the same samples may possibly compete with the infauna, suppressing the bio-irrigation behavior through constant agitation of the feeding apparatus, similar to what happens in non-lethal predator-prey interactions (Maire et al., 2010; De Smet et al., 2016). *C. fornicata* is also known to cause significant biodeposition of fine particles on the sediment surface (Ehrhold et al., 1998; Ragueneau et al., 2005). This could decrease the permeability of the surface layers and as such decrease the extent of possible bio-irrigation. Burrows of *N. latericeus* extend down to 40 cm, and they have no lining, which –in theory- would facilitate irrigation. However, the burrows are considered semi-permanent, which in turn limits the depth up to which bio-irrigation plays a role (Kikuchi, 1987; Holtmann et al., 1996). The presence of these polychaetes is thus not per se translated in high irrigation rates, though there does appear to be a link to the depth over which bio-irrigation occurs, with this being deepest in Lodijksegat (lowest *a*) where the species are present, and shallowest in Viane (highest *a*) that lacks these species.

In the intertidal stations the main species described as bio-irrigators are the mud shrimp *Corophium* sp., the lugworm *Arenicola marina* (Linnaeus, 1758), and the capitellid polychaete *Heteromastus filiformis* (Claparède, 1864). *Corophium sp.* is an active bio-irrigator that lives in lined U-shaped burrows 5 to 10 cm in depth (McCurdy et al., 2000; De Backer et al., 2010). *A. marina* is often noted as the main bio-irrigator and bioturbator in marine intertidal areas (Huettel, 1990; Volkenborn et al., 2007). This species constructs U shaped burrows of 20 to 40 cm deep, and typically injects water to this depth in irrigation bouts of 15 minutes (Timmermann et al., 2007). *H. filiformis* creates mucus-lined permanent burrows in sediments up to 30 cm deep (Aller and Yingst, 1985). These species are present in all intertidal sites presented here. High densities of *Corophium sp.* are found there where high irrigation rates are measured (Table 2 and Fig. 2: Dortsman, 6781 ± 5289 ind. m^{-2}, bio-irrigation rates between 0.942 and 1.149 mL cm^{-2} h^{-1}).

The higher abundance of previously mentioned bio-irrigators in the intertidal, as opposed to the subtidal, explains the lower attenuation coefficient values in the intertidal. Intertidal areas also experience stronger variations in physical stressors such as waves, temperature, light, salinity and precipitation than subtidal areas (Herman et al., 2001), and to biological stressors such as predation by birds (Fleischer, 1983; Granadeiro et al., 2006; Ponsero et al., 2016). Burrowing deeper, or simply residing in deeper sediment layers for a longer time, are valid strategies for species in the intertidal to combat these pressures (Koo et al., 2007; MacDonald et al., 2014).

4.3 The Bio-irrigation Potential

The Community Irrigation potential (Eq. 4, Wrede et al., 2018) subsumes both the depth of bio-irrigation and the rate. The former is represented by the injection depth (*ID*), while the latter relates to the burrowing (*BT*) and feeding type (*FT*) of the species traits scaled with their size and abundance. Interestingly, in the Oosterschelde data, only one of the irrigation parameters correlates to the IPc: the attenuation coefficient (Fig. 4c). This is most likely a consequence of the fact that the IPc index was calibrated using the Br^- linear regression method (Wrede et al., 2018), which may mainly quantify the irrigation depth. Nevertheless, the lack of a relation between the pumping rate and the IPc is surprising, since this index does include traits that are expected to affect the pumping rate, and it is scaled for metabolic activity. This suggests that bio-irrigation is a process

which not only depends on the species characteristics but also includes context dependent trait modalities that need to be considered.

Functional roles of species may differ depending on the context in which they are evaluated, and the *a priori* assignment of a species to a functional effect group may therefore be too simplistic (Hale et al., 2014; Murray et al., 2014). Christensen et al. (2000) for instance reported irrigation rates of sediments in Kertinge Nor, Denmark with high abundances of *Hediste diversicolor* (O.F. Müller, 1776) (600 ind. m^{-2} at 15 °C) that varied with a factor 4 whether the organism was suspension feeding (2704 ± 185 L m^{-2} d^{-1}) or deposit-feeding (754 ± 80 L m^{-2} d^{-1}). In our study, the intertidal station Zandkreek also had very high abundances of *H. diversicolor* (peak at 2550 ind. m^{-2} in April) but much lower irrigation rates (128.6 ± 160.6 L m^{-2} d^{-1}). Possibly, the higher Chl *a* concentrations in Zandkreek (20.2 µg gDW^{-1}) compared to the sediment in Christensen et al. (2000) (±7 µg gDW^{-1}, converted from µg gWW^{-1}) caused the species to shift even more to deposit feeding. Similarly, previously reported irrigation rates of *Lanice conchilega* in late summer were quantified to range between 26.45 and 33.55 L m^{-2} d^{-1} (3243 ± 1094 ind. m^{-2}), in an intertidal area in Boulogne-Sur-Mer, France (De Smet et al., 2016), whereas we measured rates that were more than an order of magnitude higher in the same season (229.3 ± 327.8 L m^{-2} d^{-1}; Fig. 2c), although densities were an order of magnitude lower (298 ± 216 ind. m^{-2}). *Lanice conchilega* is also known to switch from suspension-feeding to deposit-feeding when densities are lower (Buhr, 1976; Buhr and Winter, 1977). This suggests that bio-irrigation activity is higher when the *L. conchilega* is deposit feeding, although there could be of course additional context-dependent factors at play.

The species community in which an organism occurs can also affect the bio-irrigation behavior. Species regularly compete for the same source of food (e.g. filter feeders), with species changing their feeding mode to escape competitive pressure (Miron et al., 1992). Species also compete in the form of predator-prey interactions, which have also been shown to alter behavior. For example, the presence of *Crangon crangon* has been shown to reduce the food uptake of *L. conchilega* (De Smet et al., 2016), and alter the sediment reworking mode of *L. balthica* (Maire et al., 2010), in both cases because *C. crangon* preys on the feeding apparatus of these species protruding from the sediment. If bio-irrigation is to provide oxygen or to reduce the build-up of metabolites, then, given sufficient densities of other bio-irrigating organisms, oxygen halo's may overlap (Dornhoffer et al., 2012), reducing the need for individuals to pump. In Zandkreek for instance, *Arenicola marina* (Linnaeus, 1758) was present in many samples, except during summer and autumn (Fig. 2b), while *Hediste diversicolor* was present in constant densities throughout the year. Although *A. marina* is a very vigorous bio-irrigator, its presence did not lead to a doubled pumping rate, suggesting an adaptation of the ventilation behaviour to the activity of *H. diversicolor*, or vice versa. This implies that simply summing of individual species irrigation scores to obtain a bio-irrigation rate may be too simplistic.

With these considerations in mind it appears that a comprehensive understanding of the ecology of species within the appropriate spatial scale and environmental context is a prerequisite for the application of an index to predict bio-irrigation rates (and by extension other functional traits). The current index (Eq. 4) contains burrow type, feeding mode, burrow depth, and an exponent to scale the metabolic rate, but from our analysis it appears that introducing more context-dependency could improve results. In Renz et al. (2018) for example, a distinction was made between an organism's activity based on the

sediment type in which it occurred (cohesive or permeable sediment) in the calculation of their index, the Community Bioirrigation Potential (BIPc), although no comparison with measured irrigation rates has taken place. Furthermore, Wrede et al. (2018) suggested to include a temperature correction factor (Q_{10}) in the calculations to account for the expected metabolic response of macrofauna to increasing water temperatures (Brey, 2010). This temperature effect on benthic activity has indeed been noticed in similar works (Magni and Montani, 2006; Rao et al., 2014), but in our study and others the highest temperatures were not clearly associated with highest functional process rates (Schlüter et al., 2000: Braeckman et al., 2010; Queirios et al., 2015). The reasons for this ranged from a non-coincidence of the annual food pulse and the temperature peak, or the presence of confounding factors in the analysis such as faunal abundances and behavior (Forster et al., 2003).

Based on the above, we stress the importance of measuring bio-irrigation rates in field settings, as it is through repeated measurements that the complex interactions of species communities and their environment will be best understood.

5 Conclusions

By fitting fluorescent tracer measurements using a mechanistic model we were able to infer more detailed information on the bio-irrigation process in species communities than an exchange rate alone, thereby improving on linear regression techniques. Benthic organisms differ strongly in the magnitude and mode in which they express functional traits. With this study we aimed to determine whether bio-irrigation can be predicted by an index of bio-irrigation, calculated based on functional traits. This index was correlated to the attenuation coefficient, but not the bio-irrigation rate. Our findings also highlight the importance of the context in which indices for functional processes should be evaluated, because of the confounding roles of environmental conditions and behaviour. Different species assemblages can have the same bio-irrigation rates, but differ in sediment depth over which they exchange solutes. This is important to consider when implementing bio-irrigation in models of sediment biogeochemistry.

Code availability

Model code will be made available on request to the corresponding author.

Author contribution

E.D.B. developed the model and performed model simulations, performed statistical analysis, and prepared the manuscript with contributions from all co-authors. J.T. collected field data, performed measurements, and analysed macrofauna. U.B. and T.Y. contributed to the manuscript. K.S. developed and implemented the model, and contributed to the manuscript.

Competing interests

The authors declare that they have no conflict of interest.

Acknowledgements

E.D.B. is a doctoral research fellow funded by the Belgian Science Policy Office (BELSPO) BELSPO, contract BR/154/A1/FaCE-It. J.T. is a doctoral research fellow funded by the European Maritime and Fisheries Fund (EMFF), and the Netherlands Ministry of Agriculture Nature and Food Quality (LNV) (Grant/Award Number: 1300021172). U.B. is a postdoctoral research fellow at Research Foundation - Flanders (FWO, Belgium) (Grant 1201716N). We thank field technicians, and laboratory staff: Pieter Van Rijswijk, Peter van Breugel and Yvonne van der Maas, as well as students that assisted with the processing of samples: Paula Neijenhuis, Jolien Buyse, Vera Baerends. For help with the ordination methods we thank Olivier Beauchard. Lastly we thank the crew of the Research Vessel Delta.

References

Aller, R. C.: Quantifying solute distributions in the bioturbated zone of marine sediments by defining an average microenvironment, Geochim. Cosmochim. Acta, 44(12), 1955–1965, doi:10.1016/0016-7037(80)90195-7, 1980.

Aller, R. C. and Aller, J. Y.: Meiofauna and solute transport in marine muds, Limnol. Oceanogr., 37(5), 1018–1033, doi:10.4319/lo.1992.37.5.1018, 1992.

Aller, R. C. and Aller, J. Y.: The effect of biogenic irrigation intensity and solute exchange on diagenetic reaction rates in marine sediments, J. Mar. Res., 56(4), 905–936, doi:10.1357/002224098321667413, 1998.

Aller, R. C. and Yingst, J. Y.: Effects of the marine deposit-feeders Heteromastus filiformis (Polychaeta), Macoma balthica (Bivalvia), and Tellina texana (Bivalvia) on averaged sedimentary solute transport, reaction rates, and microbial distributions, J. Mar. Res., 43(3), 615–645, doi:10.1357/002224085788440349, 1985.

Andersson, J. H., Middelburg, J. J. and Soetaert, K.: Identifiability and uncertainty analysis of bio-irrigation rates, J. Mar. Res., 64(3), 407–429, doi:10.1357/002224006778189590, 2006.

De Backer, A., van Ael, E., Vincx, M. and Degraer, S.: Behaviour and time allocation of the mud shrimp, Corophium volutator, during the tidal cycle: A laboratory study, Helgol. Mar. Res., 64(1), 63–67, doi:10.1007/s10152-009-0167-6, 2010.

Beauchard, O., Veríssimo, H., Queirós, A. M. and Herman, P. M. J.: The use of multiple biological traits in marine community ecology and its potential in ecological indicator development, Ecol. Indic., 76, 81–96, doi:10.1016/j.ecolind.2017.01.011, 2017.

Berelson, W. M., Heggie, D., Longmore, a, Kilgore, T., Nicholson, G. and Skyring, G.: Benthic Nutrient Recycling in Port Phillip Bay, Australia, Estuar. coast. shelf Sci, 46, 917–934, doi:DOI: 10.1006/ecss.1998.0328, 1998.

Berg, P., Rysgaard, S., Funch, P. and Sejr, M. K.: Effects of bioturbation on solutes and solids in marine sediments, Aquat. Microb. Ecol., 26(1), 81–94, doi:DOI 10.3354/ame026081, 2001.

Braeckman, U., Provoost, P., Gribsholt, B., Van Gansbeke, D., Middelburg, J. J., Soetaert, K., Vincx, M. and Vanaverbeke, J.: Role of macrofauna functional traits and density in biogeochemical fluxes and bioturbation, Mar. Ecol. Prog. Ser., 399(2010), 173–186, doi:10.3354/meps08336, 2010.

Braeckman, U., Van Colen, C., Soetaert, K., Vincx, M. and Vanaverbeke, J.: Contrasting macrobenthic activities differentially affect nematode density and diversity in a shallow subtidal marine sediment, Mar. Ecol. Prog. Ser., 422, 179–191, doi:10.3354/meps08910, 2011.

Brey, T.: An empirical model for estimating aquatic invertebrate respiration, Methods Ecol. Evol., 1(1), 92–101, doi:10.1111/j.2041-210x.2009.00008.x, 2010.

Buhr, K.-J.: Suspension-feeding and assimilation efficiency in Lanice conchilega (Polychaeta), Mar. Biol., 38(4), 373–383, doi:10.1007/BF00391377, 1976.

Buhr, K.-J. and Winter, J. E.: Distribution and Maintenance of a Lanice Conchilega Association in the Weser Estuary (Frg), With Special Reference To the Suspension—Feeding Behaviour of Lanice Conchilega, Pergamon Press Ltd., 1977.

Christensen, B., Vedel, A. and Kristensen, E.: Carbon and nitrogen fluxes in sediment inhabited by suspension-feeding (Nereis diversicolor) and non-suspension-feeding (N. virens) polychaetes, Mar. Ecol. Prog. Ser., 192, 203–217, doi:10.3354/meps192203, 2000.

Craeymeersch, J., P, Kingston, P., Rachor, E., Duineveld, G., Heip, C. and Vanden Berghe, E.: North Sea Benthos Survey., 1986.

D'Andrea, A. F. and DeWitt, T. H.: Geochemical ecosystem engineering by the mud shrimp Upogebia pugettensis (Crustacea: Thalassinidae) in Yaquina Bay, Oregon: Density-dependent effects on organic matter remineralization and nutrient cycling, Limnol. Oceanogr., 54(6), 1911–1932, doi:10.4319/lo.2009.54.6.1911, 2009.

Degraer, S., Wittoeck, J., Appeltans, W., Cooreman, K., Deprez, T., Hillewaert, H., Hostens, K., Mees, J., Vanden Berghe, E. and Vincx, M.: Macrobel: Long term trends in the macrobenthos of the Belgian Continental Shelf. Oostende, Belgium., [online] Available from: http://www.vliz.be/vmdcdata/macrobel/, 2006.

Dornhoffer, T., Waldbusser, G. G. and Meile, C.: Burrow patchiness and oxygen fluxes in bioirrigated sediments, J. Exp. Mar. Bio. Ecol., 412, 81–86, doi:10.1016/j.jembe.2011.11.004, 2012.

Dray, S. and Dufour, A.-B.: The ade4 Package: Implementing the Duality Diagram for Ecologists, J. Stat. Softw., 22(4), doi:10.18637/jss.v022.i04, 2015.

Dray, S., Chessel, D. and Thioulouse, J.: Co-inertia analysis and the linking of ecological data tables, Ecology, 84(11), 3078–3089, doi:10.1890/03-0178, 2003.

Ehrhold, A., Blanchard, M., Auffret, J.-P. and Garlan, T.: Conséquences de la prolifération de la crépidule (Crepidula fornicata) sur l'évolution sédimentaire de la baie du Mont-Saint-Michel (Manche, France), Comptes Rendus l'Académie des Sci. - Ser. IIA - Earth Planet. Sci., 327(9), 583–588, doi:https://doi.org/10.1016/S1251-8050(99)80111-6, 1998.

Forster, S. and Graf, G.: Impact of irrigation on oxygen flux into the sediment: intermittent pumping by Callianassa subterranea and "piston-pumping" by Lanice conchilega, Mar. Biol., 123(2), 335–346, doi:10.1007/BF00353625, 1995.

Forster, S., Khalili, A. and Kitlar, J.: Variation of nonlocal irrigation in a subtidal benthic community, , (1980), 335–357, 2003.

Furukawa, Y., Bentley, S. J. and Lavoie, D. L.: Bioirrigation modeling in experimental benthic mesocosms, J. Mar. Res., 59, 417–452, doi:10.1357/002224001762842262, 2001.

Hedman, J. E., Gunnarsson, J. S., Samuelsson, G. and Gilbert, F.: Particle reworking and solute transport by the sediment-living polychaetes Marenzelleria neglecta and Hediste diversicolor, J. Exp. Mar. Bio. Ecol., 407(2), 294–301, doi:10.1016/j.jembe.2011.06.026, 2011.

Heo, M. and Gabriel, K. R.: A permutation test of association between configurations by means of the RV coefficient, Commun. Stat. Part B Simul. Comput., 27(3), 843–856, doi:10.1080/03610919808813512, 1998.

Holtmann, S. E., Groenewold, A., Schrader, K. H. M., Asjes, J., Craeymeersch, J. A., Duineveld, G. C. A., van Bostelen, A. J. and van der Meer, J.: Atlas of the zoobenthos of the Dutch continental shelf, Ministry of Transport, Public Works and Water Management, Rijswijk. [online] Available from: http://www.marinespecies.org/aphia.php?p=taxdetails&id=130644, 1996.

Huettel, M.: Influence of the lugworm Arenicola marina on porewater nutrient profiles of sand flat sediments, Mar. Ecol. Prog. Ser., 62, 241–248, doi:10.3354/meps062241, 1990.

Kikuchi, E.: Effects of the brackish deposit-feeding polychaetes Notomastus sp. (Capitellidae) and Neanthes japonica (Izuka) (Nereidae) on sedimentary O2 consumption and CO2 production rates, J. Exp. Mar. Bio. Ecol., 114(1), 15–25, doi:10.1016/0022-0981(87)90136-5, 1987.

Koo, B. J., Kwon, K. K. and Hyun, J. H.: Effect of environmental conditions on variation in the sediment-water interface created by complex macrofaunal burrows on a tidal flat, J. Sea Res., 58(4), 302–312, doi:10.1016/j.seares.2007.07.002, 2007.

Kristensen, E.: Impact of polychaetes (Nereis spp. and Arenicola marina) on carbon biogeochemistry in coastal marine sediments, Geochem. Trans., 2, 92–103, doi:10.1039/b108114d, 2001.

Kristensen, E., Penha-Lopes, G., Delefosse, M., Valdemarsen, T., Quintana, C. O. and Banta, G. T.: What is bioturbation? the need for a precise definition for fauna in aquatic sciences, Mar. Ecol. Prog. Ser., 446, 285–302, doi:10.3354/meps09506, 2012.

MacDonald, E. C., Frost, E. H., MacNeil, S. M., Hamilton, D. J. and Barbeau, M. A.: Behavioral response of Corophium

volutator to shorebird predation in the upper bay of Fundy, Canada, PLoS One, 9(10), doi:10.1371/journal.pone.0110633, 2014.

Magni, P. and Montani, S.: Seasonal patterns of pore-water nutrients, benthic chlorophyll a and sedimentary AVS in a macrobenthos-rich tidal flat, Hydrobiologia, 571(1), 297–311, doi:10.1007/s10750-006-0242-9, 2006.

Maire, O., Merchant, J. N., Bulling, M., Teal, L. R., Grémare, A., Duchêne, J. C. and Solan, M.: Indirect effects of non-lethal predation on bivalve activity and sediment reworking, J. Exp. Mar. Bio. Ecol., 395(1–2), 30–36, doi:10.1016/j.jembe.2010.08.004, 2010.

Martin, W. R. and Banta, G. T.: The measurement of sediment irrigation rates: A comparison of the Br- tracer and 222Rn/226Ra disequilibrum techniques, J. Mar. Res., 50, 125–154, doi:10.1357/002224092784797737, 1992.

McCave, I. N., Bryant, R. J., Cook, H. F. and Coughanowr, C. A.: EVALUATION OF A LASER-DIFFRACTION-SIZE ANALYZER FOR USE WITH NATURAL SEDIMENTS, J. Sediment. Res., 56, 561–564, doi:10.1306/212f89cc-2b24-11d7-8648000102c1865d, 1986.

McCurdy, D. G., Boates, J. S. and Forbes, M. R.: Reproductive synchrony in the intertidal amphipod Corophium volutator, Oikos, 88(2), 301–308, doi:10.1034/j.1600-0706.2000.880208.x, 2000.

Mestdagh, S., Bagaço, L., Ysebaert, T., Braeckman, U., De Smet, B., Moens, T. and Van Colen, C.: Functional trait responses to sediment deposition reduce macrofauna-mediated ecosystem functioning in an estuarine mudflat, Biogeosciences, 15(9), 2587–2599, doi:10.5194/bg-15-2587-2018, 2018.

Meysman, F. J. R., Galaktionov, O. S. and Middelburg, J. J.: Irrigation patterns in permeable sediments induced by burrow ventilation: A case study of Arenicola marina, Mar. Ecol. Prog. Ser., 303(November), 195–212, doi:10.3354/meps303195, 2005.

Meysman, F. J. R., Galaktionov, O. S., Gribsholt, B. and Middelburg, J. J.: Bio-irrigation in permeable sediments: An assessment of model complexity, J. Mar. Res., 64(4), 589–627, doi:10.1357/002224006778715757, 2006.

Morys, C., Powilleit, M. and Forster, S.: Bioturbation in relation to the depth distribution of macrozoobenthos in the southwestern Baltic Sea, Mar. Ecol. Prog. Ser., 579, 19–36, doi:10.3354/meps12236, 2017.

Na, T., Gribsholt, B., Galaktionov, O. S., Lee, T. and Meysman, F. J. R.: Influence of advective bio-irrigation on carbon and nitrogen cycling in sandy sediments, J. Mar. Res., 66, 691–722, doi:10.1357/002224008787536826, 2008.

Nielsen, O. I., Gribsholt, B., Kristensen, E. and Revsbech, N. P.: Microscale distribution of oxygen and nitrate in sediment inhabited by Nereis diversicolor: Spatial patterns and estimated reaction rates, Aquat. Microb. Ecol., 34(1), 23–32, doi:10.3354/ame034023, 2004.

Northeast Fisheries Science Center: Benthic Habitat Database, [online] Available from: https://catalog.data.gov/dataset/benthic-habitat-database, 2018.

Olaffson, E.: Do Macrofauna Structure Meiofauna Assemblages in Marine Soft-Bottoms ? A review of Experimental Studies, Vie Milieu, 53(4), 249–265, 2003.

Price, W. L.: A controlled random search procedure for global optimisation, Comput. J., 20(4), 367–370,

doi:10.1093/comjnl/20.4.367, 1977.

Queirios, A. M., Stephens, N., Cook, R., Ravaglioli, C., Nunes, J., Dashfield, S., Harris, C., Tilstone, G. H., Fishwick, J., Braeckman, U., Somerfield, P. J. and Widdicombe, S.: Can benthic community structure be used to predict the process of bioturbation in real ecosystems?, Prog. Oceanogr., 137(April), 559–569, doi:10.1016/j.pocean.2015.04.027, 2015.

Queirós, A. M., Birchenough, S. N. R., Bremner, J., Godbold, J. A., Parker, R. E., Romero-Ramirez, A., Reiss, H., Solan, M., Somerfield, P. J., Van Colen, C., Van Hoey, G. and Widdicombe, S.: A bioturbation classification of European marine infaunal invertebrates, Ecol. Evol., 3(11), 3958–3985, doi:10.1002/ece3.769, 2013.

Quintana, C. O., Tang, M. and Kristensen, E.: Simultaneous study of particle reworking, irrigation transport and reaction rates in sediment bioturbated by the polychaetes Heteromastus and Marenzelleria, J. Exp. Mar. Bio. Ecol., 352(2), 392–406, doi:10.1016/j.jembe.2007.08.015, 2007.

R Core Team: R: A language and environment for statistical computing, [online] Available from: http://www.r-project.org/, 2013.

Ragueneau, O., Chauvaud, L., Moriceau, B., Leynaert, A., Thouzeau, G., Donval, A., Le Loc'h, F. and Jean, F.: Biodeposition by an invasive suspension feeder impacts the biogeochemical cycle of Si in a coastal ecosystem (Bay of Brest, France), Biogeochemistry, 75(1), 19–41, doi:10.1007/s10533-004-5677-3, 2005.

Rao, A. M. F., Malkin, S. Y., Montserrat, F. and Meysman, F. J. R.: Alkalinity production in intertidal sands intensified by lugworm bioirrigation, Estuar. Coast. Shelf Sci., 148, 36–47, doi:10.1016/j.ecss.2014.06.006, 2014.

Renz, J. R., Powilleit, M., Gogina, M., Zettler, M. L., Morys, C. and Forster, S.: Community bioirrigation potential (BIP c), an index to quantify the potential for solute exchange at the sediment-water interface, Mar. Environ. Res., (July), 0–1, doi:10.1016/j.marenvres.2018.09.013, 2018.

Ritchie, R. J.: Consistent sets of spectrophotometric chlorophyll equations for acetone, methanol and ethanol solvents, Photosynth. Res., 89(1), 27–41, doi:10.1007/s11120-006-9065-9, 2006.

Rysgaard, S., Christensen, P. B., Sørensen, M. V., Funch, P. and Berg, P.: Marine meiofauna , carbon and nitrogen mineralization in sandy and soft sediments of Disko Bay, West Greenland, Aquat. Microb. Ecol., 21, 59–71, doi:10.3354/ame021059, 2000.

Schlüter, M., Sauter, E., Hansen, H. P. and Suess, E.: Seasonal variations of bioirrigation in coastal sediments: Modelling of field data, Geochim. Cosmochim. Acta, 64(5), 821–834, doi:10.1016/S0016-7037(99)00375-0, 2000.

Sistermans, W. C. H., Hummel, H., Dekker, A. and Dek, L. A.: Inventarisatie macrofauna Westerschelde Najaar 2005, Yerseke., 2006.

De Smet, B., Braeckman, U., Soetaert, K., Vincx, M. and Vanaverbeke, J.: Predator effects on the feeding and bioirrigation activity of ecosystem-engineered Lanice conchilega reefs, J. Exp. Mar. Bio. Ecol., 475, 31–37, doi:10.1016/j.jembe.2015.11.005, 2016.

Soetaert, K. and Petzoldt, T.: Inverse Modelling, Sensitivity and Monte Carlo analysis in R Using PAckage FME, J. Stat. Softw., 33(3), 1–28, doi:10.18637/jss.v033.i03, 2010.

Soetaert, K., Petzoldt, T. and Setzer, R. W.: Solving Differential Equations in R : Package deSolve, J. Stat. Softw., 33(9), doi:10.18637/jss.v033.i09, 2010.

Solan, M., Cardinale, B. J., Downing, A. L., Engelhardt, K. A. M., Ruesink, J. L. and Srivastava, D. S.: Extinction and Ecosystem Funciton in the Marine Benthos, Science (80-.)., 306(2004), 1177–1180, doi:10.1126/science.1103960, 2004.

Tenenhaus, M. and Young, F. W.: An analysis and synthesis of multiple correspondence analysis, optimal scaling, dual scaling, homogeneity analysis and other methods for quantifying categorical multivariate data, Psychometrika, 50(1), 91–119, doi:10.1007/BF02294151, 1985.

Thioulouse, J., Dray, S., Dufour, A.-B., Siberchicot, A., Jombart, T. and Pavoine, S.: Multivariate Analysis of Ecological Data, 1st ed., Springer-Verlag New York, New York., 2018.

Timmermann, K., Banta, G. T. and Glud, R. N.: Linking Arenicola marina irrigation behavior to oxygen transport and dynamics in sandy sediments, J. Mar. Res., 64(6), 915–938, doi:10.1357/002224006779698378, 2007.

Volkenborn, N., Hedtkamp, S. I. C., van Beusekom, J. E. E. and Reise, K.: Effects of bioturbation and bioirrigation by lugworms (Arenicola marina) on physical and chemical sediment properties and implications for intertidal habitat succession, Estuar. Coast. Shelf Sci., 74(1–2), 331–343, doi:10.1016/j.ecss.2007.05.001, 2007.

Warren, L. M.: The Ecology of Capitella capitata in British Waters, J. Mar. Biol. Assoc. United Kingdom, 57(1), 151–159, doi:10.1017/S0025315400021305, 1977.

Wrede, A., Beermann, J., Dannheim, J., Gutow, L. and Brey, T.: Organism functional traits and ecosystem supporting services – A novel approach to predict bioirrigation, Ecol. Indic., 91(April), 737–743, doi:10.1016/j.ecolind.2018.04.026, 2018a..

Figures

Figure 1: Subtidal (white dots) and intertidal (black dots) sampling stations in the Oosterschelde estuary.

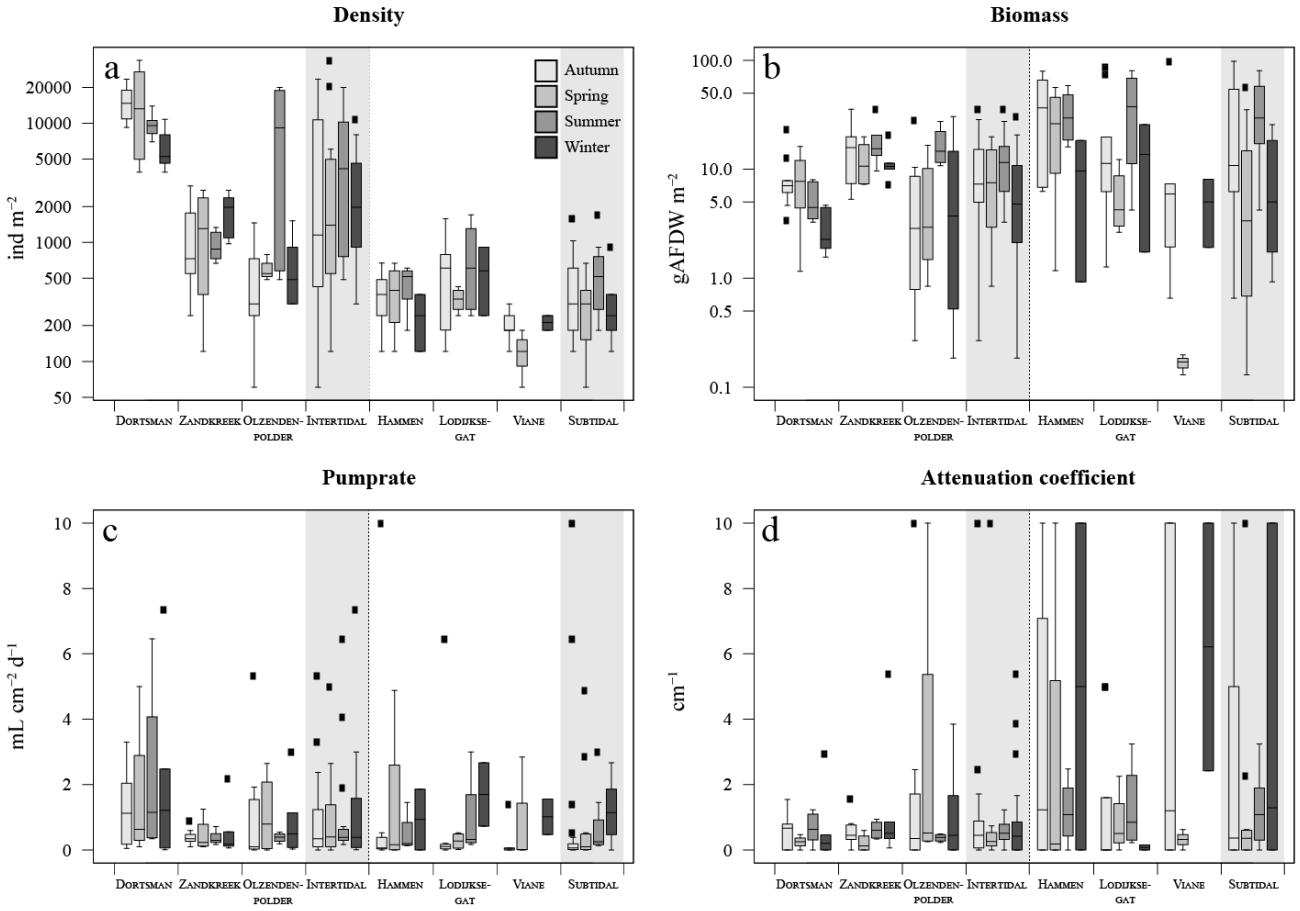

590 **Figure 2: (a) organism densities (ind m^{-2}); (b) organism biomass as ash-free dry weight (gAFDW m^{-2}); (c) model derived pumping rate (mL cm^{-2} d^{-1}); (d) model derived attenuation coefficient (cm^{-1}). Data arranged per station (white areas) and per habitat type, intertidal and subtidal (grey shaded areas). Black squares = outliers.**

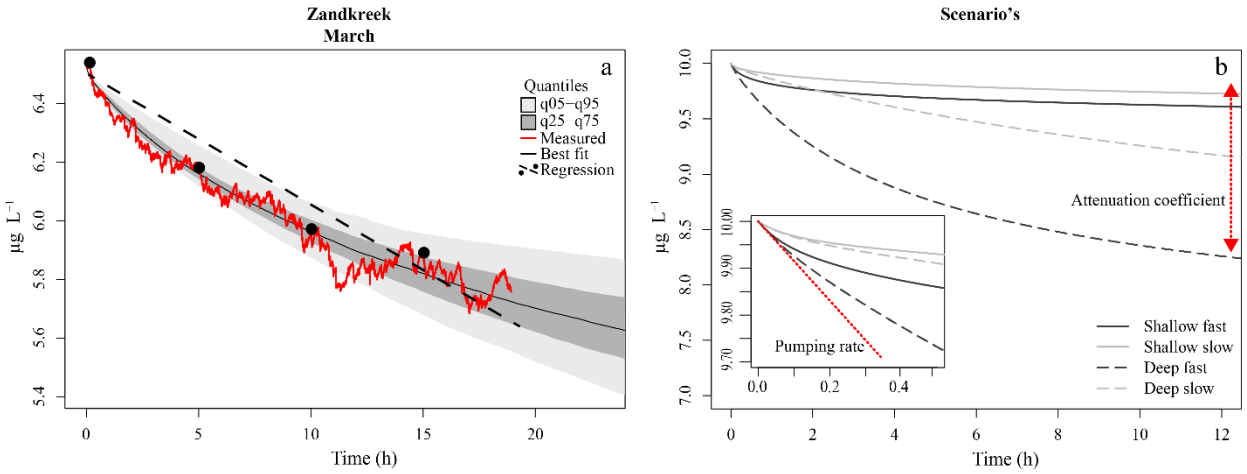

Figure 3: (a) Model fit to data (red line) from a core at Zandkreek in March 2017. The best fit tracer profile (full black line) is shown, along with the range of model outputs as quantiles (light and dark grey). An example of a linear fit (dashed line) through (fictitious) samples taken every 5 hours (dots) is also shown. (b) Example model output for different combinations of pumping rate (slow = 0.15 mL cm^{-2} h^{-1} , fast = 0.8 mL cm^{-2} h^{-1}), and attenuation coefficients (shallow = 5 cm^{-1}- deep = 0.5 cm^{-1}). The inset shows a close-up of the first half hour of the simulation. Red line illustrates the effect of the pumping rate, which has the strongest initial effect; red arrow illustrates the effect of the attenuation coefficient, which determines the depth of the irrigation.

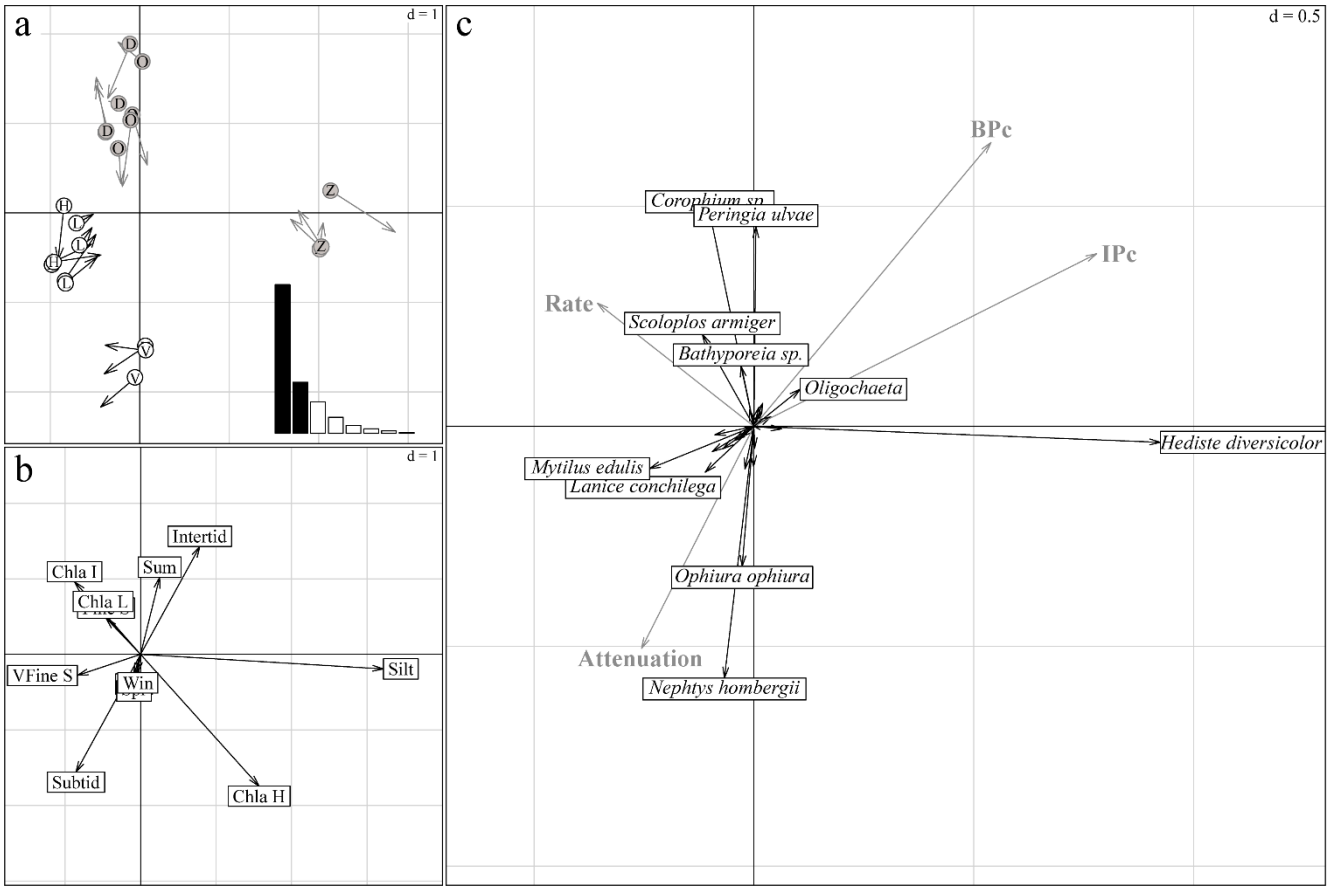

Figure 4: Summary of the coinertia analysis (CoIA). (a) Co-structure between abiotic samples (circles) and species samples (arrow tips); grey circles "D", "O","Z" for intertidal sites Dortsman, Olzendenpolder and Zandkreek respectively; white circles "H", "L", "V" for subtidal sites Hammen, Lodijksegat and Viane respectively. Arrow length corresponds to the dissimilarity between the abiotic data and the species data (the larger the arrow, the larger the dissimilarity). Pearson's correlation between the circle and arrow tip coordinates on the first axis: r = 0.95, p < 0.001; on the second axis, r = 0.92, p < 0.001. Sites are more similar in terms of environmental conditions (circles), or species (arrow tips), when they group closer together. Inset: eigenvalue diagram of the co-structure; first axis explains 57%, second axis explains 19% of the variation in the dataset. (b) MBA based on environmental variables. (c) Species projections (dark arrows) and projected response variables (bio-irrigation parameters and bioturbation and bio-irrigation index) onto the co-inertia axes (grey arrows). The directions of arrows in figures b and c corresponds to the directions in which stations are grouped in terms of abiotic data (circles) and species composition (arrow tips) in figure a.

Tables

Table 1: Sampling frequency of the different research sites, and average seasonal temperature of the water in the incubation cores during the measurements

Season	Spring	Summer	Autumn	Winter
Months	Apr – Jun	Jul – Sep	Oct – Dec	Jan – Mar
Avg. Temperature (°C)	12.8	17.9	11.9	7.3
Dortsman	4	5	9	5
Zandkreek	4	6	9	6
Olzendenpoder	4	4	8	6
Lodijksegat	4	4	8	2
Hammen	4	4	8	2
Viane	3	0	6	2

Table 2: Sediment characteristics averaged over the study period (n= 8 per sampling site) represented with standard deviation for the intertidal sites Dortsman, Olzendenpolder and Zandkreek, and the subtidal sites Lodijksegat, Hammen and Viane.

	Dortsman	Olzendenpolder	Zandkreek	Lodijksegat	Hammen	Viane
% Silt	0 ± 0	14 ± 16	51 ± 7	25 ± 5	24 ± 5	63 ± 19
CN ratio (mol mol^{-1})	6.5 ± 1.2	11.3 ± 2.4	9.3 ± 1.0	12.4 ± 1.4	9.8 ± 0.9	9.9 ± 1.0
% C_{org}	0.07 ± 0.02	0.30 ± 0.27	0.79 ± 0.33	0.58 ± 0.12	0.35 ± 0.07	1.16 ± 0.36
d50 (µm)	140 ± 2	112 ± 24	59 ± 14	116 ± 7	201 ± 38	53 ± 60
Porosity (-)	0.43 ± 0.07	0.53 ± 0.07	0.45 ± 0.09	0.52 ± 0.03	0.45 ± 0.03	0.73 ± 0.06
***Chl* a (µg g^{-1})**	8.65 ± 3.53	9.97 ± 2.80	20.60 ± 4.19	5.33 ± 3.92	3.76 ± 2.43	10.26 ± 3.92

Table 3: Species densities per station and per season (ind m^{-2}), excluding species that were only encountered once.

	Species	Autumn	Spring	Summer	Winter	Annual
Dortsman Intertidal	*Arenicola marina*	113 ± 74	440 ± 395	91 ± 35	0	194 ± 244
	Bathyporeia sp.	1789 ± 1381	3934 ± 3087	1443 ± 1452	577 ± 350	1735 ± 1833
	Capitella capitata	289 ± 416	223 ± 153	304 ± 0	73 ± 27	192 ± 240
	Cerastoderma edule	61 ± 0	61 ± 0	61 ± 0	81 ± 35	69 ± 23
	Corophium sp.	9957 ± 4465	7120 ± 9205	5848 ± 2792	2977 ± 1850	6781 ± 5289
	Eteone longa	61 ± 0	0	122 ± 0	61 ± 0	85 ± 33
	Hediste diversicolor	91 ± 61	547 ± 687	304 ± 182	61 ± 0	243 ± 311
	Limecola balthica	122 ± 0	0	152 ± 43	61 ± 0	109 ± 51
	Nematoda	0	273 ± 129	61 ± 0	0	203 ± 153
	Oligochaeta	219 ± 164	851 ± 0	1175 ± 1719	122 ± 50	458 ± 839
	Peringia ulvae	1409 ± 1538	365 ± 0	658 ± 729	840 ± 381	911 ± 933
	Pygospio elegans	425 ± 0	0	0	61 ± 0	134 ± 163
	Scoloplos armiger	1782 ± 1197	1470 ± 1195	1288 ± 691	1580 ± 970	1572 ± 1013

	Scrobicularia plana	1175 ± 460	608 ± 662	759 ± 301	61 ± 0	753 ± 570
	Tellinoidea	61 ± 0	61 ± 0	0	61 ± 0	61 ± 0
Zandkreek Intertidal	*Abra alba*	76 ± 30	152 ± 43	91 ± 43	61 ± 0	95 ± 44
	Arenicola marina	61 ± 0	152 ± 43	0	0	122 ± 61
	Hediste diversicolor	1013 ± 737	1409 ± 780	1033 ± 392	1326 ± 520	1156 ± 609
	Heteromastus filiformis	0	182 ± 0	0	76 ± 30	97 ± 54
	Oligochaeta	324 ± 175	0	0	375 ± 383	358 ± 316
	Tharyx sp.	61 ± 0	0	0	91 ± 43	81 ± 35
Olzendenpolder Intertidal	*Arenicola marina*	142 ± 93	122 ± 105	122 ± 105	122 ± 0	128 ± 83
	Capitella capitata	61 ± 0	101 ± 35	61 ± 0	0	85 ± 33
	Cerastoderma edule	61 ± 0	61 ± 0	61 ± 0	0	61 ± 0
	Crangon crangon	0	61 ± 0	122 ± 0	0	76 ± 30
	Hediste diversicolor	61 ± 0	61 ± 0	0	182 ± 0	122 ± 70
	Heteromastus filiformis	0	122 ± 0	0	61 ± 0	101 ± 35
	Notomastus sp.	81 ± 35	61 ± 0	61 ± 0	152 ± 78	108 ± 66
	Oligochaeta	0	122 ± 0	152 ± 43	213 ± 215	170 ± 117
	Peringia ulvae	61 ± 0	0	12454 ± 10795	304 ± 86	6339 ± 9566
	Polydora ciliata	122 ± 0	0	0	61 ± 0	101 ± 35
	Scoloplos armiger	344 ± 220	410 ± 135	182 ± 105	279 ± 213	314 ± 188
	Tharyx sp.	243 ± 61	0	0	61 ± 0	152 ± 107
Hammen Subtidal	*Actiniaria*	144 ± 72	97 ± 54	134 ± 51	61 ± 0	125 ± 62
	Ensis sp.	61 ± 0	0	61 ± 0	0	61 ± 0
	Hemigrapsus sp.	61 ± 0	0	122 ± 0	0	81 ± 35
	Mytilus edulis	61 ± 0	3311 ± 215	2886 ± 2105	0 ± 0	2491 ± 1735
	Nephtys hombergii	85 ± 33	61 ± 0	61 ± 0	61 ± 0	71 ± 24
	Notomastus sp.	111 ± 81	203 ± 93	152 ± 43	61 ± 0	137 ± 82
	Ophiura ophiura	122 ± 0	0	243 ± 161	0	213 ± 145
	Scoloplos armiger	0	61 ± 0	0	91 ± 43	81 ± 35
	Terebellidae	61 ± 0	61 ± 0	61 ± 0	0 ± 0	61 ± 0
Lodijksegat Subtidal	*Crepidula fornicata*	319 ± 152	122 ± 0	972 ± 172	0	477 ± 369
	Hemigrapsus sp.	61 ± 0	0	61 ± 0	0	61 ± 0
	Lanice conchilega	375 ± 225	304 ± 0	91 ± 43	273 ± 301	298 ± 216
	Malmgrenia darbouxi	91 ± 43	0	0	182 ± 0	122 ± 61
	Nephtys hombergii	111 ± 60	158 ± 92	0	0	133 ± 76
	Notomastus sp.	81 ± 35	91 ± 43	61 ± 0	61 ± 0	78 ± 30
	Pholoe baltica	61 ± 0	0	122 ± 0	61 ± 0	76 ± 30
	Scoloplos armiger	122 ± 0	61 ± 0	122 ± 0	122 ± 0	106 ± 30
	Terebellidae	31 ± 42	0	0	61 ± 0	41 ± 34
Viane Subtidal	*Nephtys hombergii*	162 ± 93	101 ± 70	0	122 ± 0	129 ± 68
	Ophiura ophiura	167 ± 58	0	0	91 ± 43	142 ± 63

Table 4: Seasonally averaged values for Chl a in the upper 2 cm of the sediment (µg Chl a g^{-1}), species density (ind m^{-2}), biomass (gAFDW m^{-2}), pumping rate (mL cm^{-2} h^{-1}), and the attenuation coefficient (cm^{-1}) for the intertidal and the subtidal.

	Season	Chl *a*	Individual density	Biomass	Pump rate	Attenuation
Intertidal	Autumn	12.49 ± 6.92	5828 ± 7509	11.16 ± 9.31	0.88 ± 1.24	0.97 ± 1.91
	Spring	12.30 ± 3.89	6005 ± 10421	8.72 ± 6.48	1.03 ± 1.48	1.09 ± 2.81
	Summer	14.69 ± 6.58	6193 ± 6763	13.65 ± 8.91	0.72 ± 1.02	0.59 ± 0.34
	Winter	14.17 ± 7.52	2645 ± 2702	8.02 ± 8.10	0.79 ± 0.96	1.05 ± 1.56
Subtidal	Autumn	5.90 ± 4.37	439 ± 365	25.67 ± 30.42	0.16 ± 0.31	2.96 ± 3.91
	Spring	7.00 ± 3.00	298 ± 181	12.15 ± 18.08	0.83 ± 1.58	1.33 ± 2.95
	Summer	4.20 ± 2.27	623 ± 494	36.67 ± 26.29	0.73 ± 1.02	1.23 ± 1.14
	Winter	6.02 ± 7.08	344 ± 289	9.45 ± 10.32	1.22 ± 0.99	3.76 ± 4.92

Table 5: Pearson correlations of the response variables against the ordination axes of the coinertia analysis, with *p*-values reported under the values in italics.

	Irrigation *r*	Attenuation *a*	BPc	IPc
	mL cm^{-2} h^{-1}	cm^{-1}	$gWW^{0.5}$ m^{-2}	$gAFDW^{0.75}$ m^{-2}
Axis 1	-0.345	-0.288	0.540	0.780
	0.107	*0.182*	*0.008*	*< 0.001*
Axis 2	0.263	-0.565	0.646	0.395
	0.226	*0.005*	*< 0.001*	*0.062*